6A.4 ASYMMETRIC STRUCTURE and MAINTENANCE in HURRICANE JUAN

Weiqing Zhang[1,2] , William Perrie*[1,2]

[1]Fisheries & Oceans Canada, Bedford Institute of Oceanography, Dartmouth, Canada
[2]Dept. Engineering Mathematics, Dalhousie University, Halifax, Canada

1. Introduction

When tropical cyclones (TCs) move polarward, mid-latitude circulation plays a very important role in their evolution, and the processes related to extratropical transition (ET), dissipation or reintensification. What makes Juan (September 2003) interesting is that it did not undergo an immediate transformation and reintensification as it moved to the extratropics. Rather, it retained a strong tropical hurricane structure with sustained category 2 hurricane intensity, almost until landfall. In this study, Juan is simulated by the Canadian Mesoscale Compressible Community (MC2 version 4.9.3) atmospheric model, using a vortex initialization. We show that when Juan stays south of the Gulf Stream, its cyclone circulation is a main source of its maintenance and its structure is almost symmetric. Thereafter, until landfall, the interaction between the cyclone's circulation and the midlatitude intense high pressure system to the northeast, dominates Juan's evolution in the form of a low-level strong south-southeastern jet as well as enhanced warm advection ahead of the surface cyclone. Storm structure is quite asymmetric due to the asymmetric convection within the associated deep saturated air mass. Although a broad low system is located to the northwest of Juan, it is relatively distant due to blocking by the intense high pressure system to the northeast, and its direct influence is negligible. Understanding Juan's development is needed in ongoing studies and simulations of ocean surface waves and currents.

2. Synoptic diagnosis

Juan reached hurricane strength by 12 UTC 26 Sept. and intensified to maximum wind intensity of 90 knots, and minimum SLP of 969 hPa, at 18 UTC 27 Sept. north of Bermuda (NHC / CHC Canadian Hurricane Centre). Moving towards Nova Scotia with sustained SLP of 970 hPa, its intensity began to weaken due to the cooler shelf waters south of Nova Scotia (Fig. 1a). However, because of its accelerating translational speed, Juan spent little time over these cooler waters and did not weaken significantly. It made landfall near Halifax (03 UTC 29 Sept.), with winds of 85 knots and minimum SLP of 973 hPa. A high-amplitude low to the west and an intense high to the east propelled Juan across central Nova Scotia to the Gulf of St. Lawrence where it weakened and was absorbed by an extratropical low.

*Corresponding author address: William Perrie, Bedford Institute of Oceanography, Dartmouth, Nova Scotia, Canada; Phone 902-426-3985; E-mail: perriew@mar.dfo-mpo.gc.ca.

3. Methods

The MC2 model is a nonhydrostatic, fully elastic, state-of-the-art model. Three-dimensional semi-Lagrangian advection and a semi-implicit time stepping are used to solve the primitive Euler equations. The turbulent vertical diffusion scheme developed by Mailhot and Benoit (1982) uses turbulent kinetic energy to specify a diffusion-type transfer coefficient, which is particularly important in the boundary layer. The surface heat and moisture fluxes over land are calculated from a force-restore scheme, as described by Benoit et al. (1997), with sea surface temperatures prescribed by weekly means. The Kain-Fritsch scheme (Kain and Fritsch, 1993) is used for deep cumulus convection. The cloud water scheme of Sundqvist et al. (1989) is used for the condensation process.

The model is implemented on a latitude-longitude grid, on 40°W - 90°W and 25°N - 59°N, with 30 vertical layers. The lowest level is 18 m, the horizontal resolution is 0.2°, and the time step is 600s. Simulations are initialized at 18 UTC 27 Sept., using the CMC (Canadian Meteorological Center) regional data assimilation system. MC2 interpolates linearly between analyses to obtain boundary conditions for every step.

Because the CMC analysis data are weak compared with the forecasted results, we insert a bogus vortex circulation (following Davidson et al.; 1992, 1993) to give an accurate initial location and storm structure to initialize our simulations. The bogus structure is defined by the storm strength,

size and position from NHC data. The initial SLP at the hurricane center (63.2°W, 35.5°N) is set to 969 hPa, and the radius of 20 m s^{-1} winds is 250 km.

Using the initialization bogus, the resultant (denoted MC2-bogus) simulated storm track is in good agreement with the analysis storm track compared to the baseline simulation (MC2 only), particularly for the first 12 h (Fig. 1a). Associated maximal surface winds agree well with NCEP/QSCAT (http://dss.ucar.edu/datasets/ds744.4/) (Fig. 1b). However, both simulated and NCEP/QSCAT winds differ from the NHC analysis data by ~ 15 ms^{-1}, which is significant. Possible reasons for our bias may be errors in pressure gradients and the radii of curvature.

4. Mesoscale structure before landfall

4.1 Model comparison with observations

From 0115 UTC 29 to 0326 UTC 29 Sept. prior to Juan's landfall, the National Research Council of Canada Convair-580 aircraft deployed 11 dropsondes along the storm track and 23 dropsondes across the storm track. There were two eye penetrations – one on the south-bound along-track section, and another on the northeast-bound across-track section (Fig. 2).

A notable feature in the dropsonde data is the asymmetric wind structure. The cross - track (Fig. 3a) wind speed to the right (east) of the storm center is almost twice the magnitude of that of the left (west) side. A very deep layer of high winds, in excess of 40 m s^{-1}, occurs as high as the 500 hPa level. On the along - track section (Fig. 3b), maximal wind speed is 47.5 m s^{-1}, and to the north of storm center, above 800 hPa, the wind decreases quickly.

Along the storm track, MC2-bogus simulation (Fig. 3d) successfully estimated the location and magnitude of the maximum observed wind speed, as well as the rapid reduction that occurs above 800 hPa. However, our model was unable to represent some of the details recorded by dropsonde 6, because the vertical resolution of the model is not fine enough, compared to dropsonde data. In the cross-track direction, the simulation (Fig. 3c) succeeded in estimating an asymmetric wind structure, with the maximum winds up to 55 ms^{-1}, which is consistent with the observations. However, this maximum wind center slightly deviates to the east, compared to observations, by about 50~100 km due to storm track bias (Fig 1a).

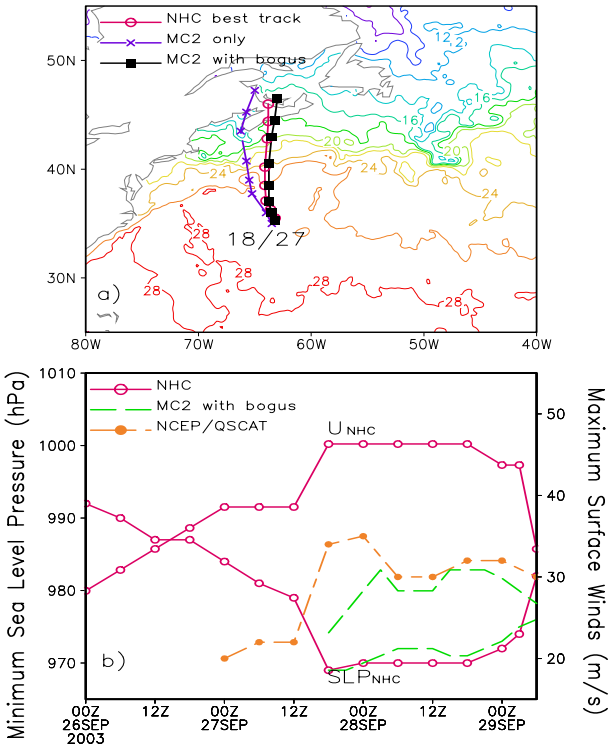

Figure 1. Comparison of storm track (a) and minimum sea level pressure and maximum surface winds (b) start from 1800 UTC 27 between simulations and NHC results. Superposed contours in (a) are daily averaged SST at 28 September from Advanced Data Fusion Center Modular Ocean Data Assimilation System.

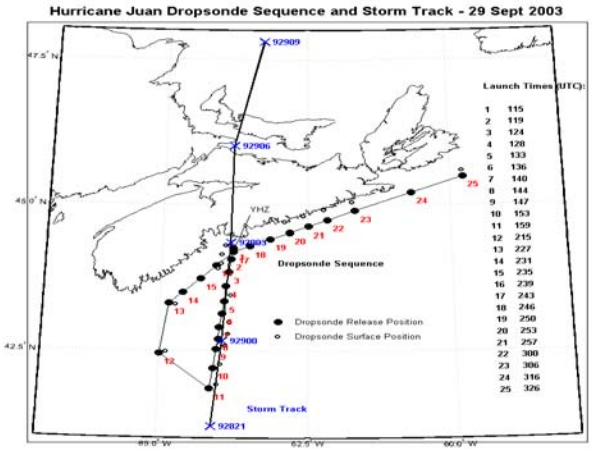

Figure 2 Convair flight and dropsonde release pattern with storm track.

Regarding equivalent potential temperature (θe), the observed south-north along-track vertical section (Fig. 4a) shows a high-θe tube that tilts cyclonically upward from low-level in the south to

mid-level in the north, due to the strong swirling flow. It is maximal above 700 hPa as a result of latent heat release. In the west-east cross-track vertical section, a vertical high-θe chimney (Fig. 4b) occurs just to the west of the storm center, rather than to the east of the storm center, as was the case for wind speed. Figure 4c shows relatively dry air to the west, and suggests that a lower-level high temperature center (between 950 and 850 hPa) and a mid-level warm ridge (~dropsonde16) just to the west of storm center, are directly responsible for the high-θe west chimney, since an associated upward chimney of relative humidity also occurs to the east of storm center (not shown).

4.2 Asymmetric structure and maintenance

Earlier studies show that higher vertical shear (Kimball and Evans, 2002; Frank and Ritchie, 2001), boundary layer convergence (Shapiro, 1992), asymmetric relative flow (Bender, 1997; Frank and Ritchie, 1999), and vortex stretching and compression mechanisms (Willoughby et al., 1984) are possible hypotheses to explain asymmetric structures. We examine these mechanisms and their possible contributions to Juan's asymmetric structure and maintenance.

A strong wind shear region, inferred from the vertical shear between 850 and 200 hPa (Fig. 6a) within the domain indicated by the 1000×1000 km box in Fig. 5b, occurs to the north of Juan, and results from the directional wind shear (Figs. 5a and 6c); the low wind shear area, indicative of the storm's center (with < 10 m s^{-1}), occupies only a small area of radius of ~50 km. Although Juan is categorized as a tropical cyclone, because it is moving over a midlatitude extratropical area, the conventional vertical levels of 200 and 850 hPa used to estimate vertical shear in tropical cyclones may not be appropriate. One concern is that above 400 hPa the storm system begins to tilt northeasterly with altitude, due to the intensifying influence of the high level jet (HLJ), in Figs. 5a-5c.

If the vertical difference between levels 400 and 850 hPa is used to define vertical shear, then vertical shear around Juan's center is clearly asymmetric (Fig. 6b) at 03 UTC 29, and the storm center is encircled by southwestern lower shear (<12 m s^{-1}) and northeastern higher shear. An explanation for the effect of higher vertical shear on asymmetric storm structure is given by Frank and Ritchie (2001) regarding the response of a storm to the imbalances caused by shear. Moreover, because of the ventilation of the hurricane warm core, higher vertical shear has negative impact on storm intensification (Kimball and Evans; 2002). According to this explanation, higher asymmetric vertical wind shear features contribute to Juan's asymmetric structure, but they are not favorable for its maintenance.

Recently, Zhu et al. (2004) suggested that the relationship between intensification in tropical cyclones and vertical wind shear is more complex than suggested by earlier "ventilation" hypotheses. Moreover, these hypotheses do not seem to be applicable to all the hurricane cases; the impact of environmental flow on the hurricane needs to be considered. Checking the vertical distribution of horizontal winds within the domain of the wind shear calculation (indicated by the box in Figs. 5b and 6c) suggests that the south-southwesterly jet in the eastern quadrant at 850 hPa has a negative vertical speed shear. This plays an important role in transporting high-θe air (shown in Figs. 5c) and cyclonic angular momentum into the system (Zhu, et al., 2004). Moreover, the low-level convergence related to the increased easterly flow at the surface (Fig. 6c) tends to moisten and destabilize the storm's eastern side, which leads to strong ascending motion, and intensification at the mid-level, due to latent heat release.

In contrast to the eastern quadrant, the upper-level convergence (see Fig. 5a) to the rear-left side of the storm (situated on the right side of the upper level jet stream where wind speed is reduced) induces a descending inflow into the western portion of the system (Fig. 5b and 6c). Associated maximal subsidence is at about 700 hPa. This descending inflow with dryer intrusion air tends to suppress the local cloud development (Fig. 6c), showing relative humidity less than 80%. These processes represent favorable conditions in the eastern quadrant which overcompensate the negative effects in the western quadrant. Therefore, at this time, intense convection tends to be organized on the east side of the storm, driven by asymmetric vertical motion associated with the environmental inflow; the southeastern component from the subtropical high is notable and should constitute the main contribution.

5. Summary and Conclusions

We simulated a weak category 2 hurricane Juan from 18 UTC 27 to 18 UTC 29 Sept. using the MC2 model, and a bogus initialization vortex, and compared simulated mesoscale features with observed dropsonde data. Understanding Juan's development is needed in ongoing studies and

simulations of ocean surface waves and currents. Simulations reproduce the storm track reasonably well, and also produce intensity and asymmetric structure before landfall that are generally consistent with the observed storm data.

In the first stage of the simulation, the hurricane itself provides more support for its maintenance in the form of its own thermodynamic structure and upper-level outflow dynamic influence. In the (second) transition stage before landfall, the interaction between the cyclone's circulation and the high pressure system dominates the storm's maintenance. Apparently, the interaction between midlatitude circulation and tropical cyclones is sufficiently complex that even an unfavorable pattern can still allow transition to occur under the proper conditions. By comparison, the upstream trough, a potentially favorable pattern for TC reintensification after the system has moved to extratropical latitudes, is distant due to blocking by the high pressure system. Thus, baroclinic influences are weak compared to other ET mechanisms, and transition does not occur.

Acknowledgments

We would like to thank Chris Fogarty for providing access to the dropsonde data presented in Figs. 3a-3b. Support is from the Canadian Panel on Energy Research and Development (Offshore Environmental Factors Program), ONR (US Office of Naval Research) via GoMOOS - the Gulf of Maine Ocean Observing System, Petroleum Research Atlantic Canada (PRAC), and the CFCAS (Canadian Foundation for Climate and Atmospheric Studies) and the Natural Sciences and Engineering Research Council of Canada.

References

Bender, M., 1997: The effect of relative flow on the asymmetric structure in the interior of hurricanes. *J. Atmos. Sci.*, 54, 703-724.

Benoit, R., M. Desgagne, P. Pellerin, Y. Chartier, and S. Desjardins, 1997: The Canadian MC2: A semi-implicit semi-Lagrangian wide-band atmospheric model suited for fine-scale process studies and simulation. *Mon. Wea. Rev.*, **125**, 2382-2415.

Davidson, N. E., and K. Puri, 1992: Tropical prediction using dynamic nudging, satellite-defined convective heat sources, and a cyclone bogus. *Mon. Wea. Rev.*, **120**, 2501-2522.

_____, J. Wadsley, and K. Puri, 1993: Implementation of the JMA typhoon bogus in the BMRC tropical prediction system. *J. Meteor. Soc. Japan*, **71**, 438-467.

Frank, W. M., and E. A., Ritchie, 1999:Effects of environment flow upon tropical cyclone structure. *Mon. Wea. Rev.*, **127**, 2044-2061.

_____, and _____, 2001: Effects of vertical wind shear on hurricane intensity and structure. *Mon. Wea. Rev.*, **129**, 2249-2269.

Kain, J.S., and J. M. Fritsch, 1993: Convective parameterization for mesoscale models: The Kain-Fritsch scheme. The representation of cumulus convection in numerical models, K. A. Emanuel and D.J. Raymond, Eds., Amer. Meteor. Soc., 246 pp.

Kimball, S. K., and Evans, J. L., 2002: Idealized numerical simulation of hurricane-trough interaction. *Mon. Wea. Rev.*, **130**, 2210-2227.

Mailhot, J., and R. Benoit, 1982: A finite-element model of the atmospheric boundary layer suitable for use with numerical weather prediction models. *J. Atmos. Sci.*, **39**, 2249-2266.

Shapiro, L. J., 1992: Hurricane vortex motion and evolution in a three-layer model. *J. Atmos. Sci.*, 49, 140-153.

Willoughby, H. E., F. D., Marks, and R. J. Feinberg, 1984: Stationary and moving convective bands in hurricanes. *J. Atmos. Sci.*, 41, 3189-3211.

Zhu, T., D.-L. Zhang, and F. Weng, 2004: Numerical simulation of hurricane Bonnie (1998). Part I: eyewall evolution and intensity changes. *Mon. Wea. Rev.* **132**, 225-241.

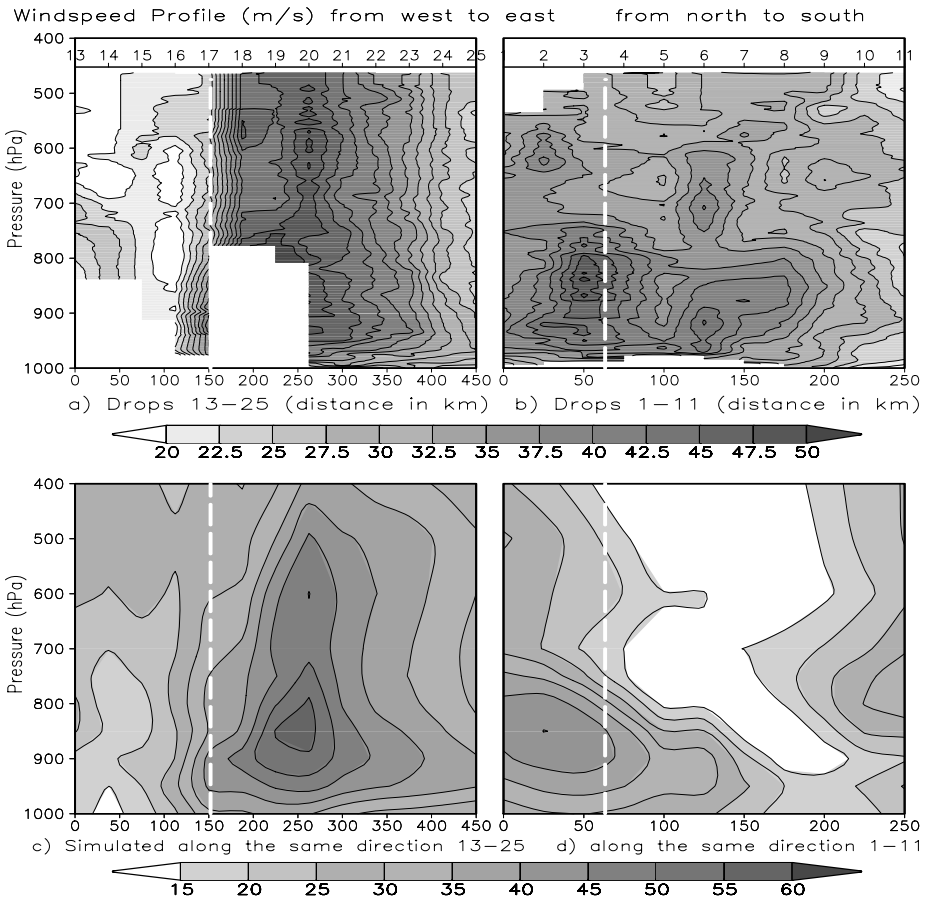

Figure 3. Vertical cross section of wind speeds along dropsondes 13-25 for (a) observation and (c) simulation, (b) and (d) for observation and simulation along dropsondes 1-11. Dashed line indicates the storm centre.

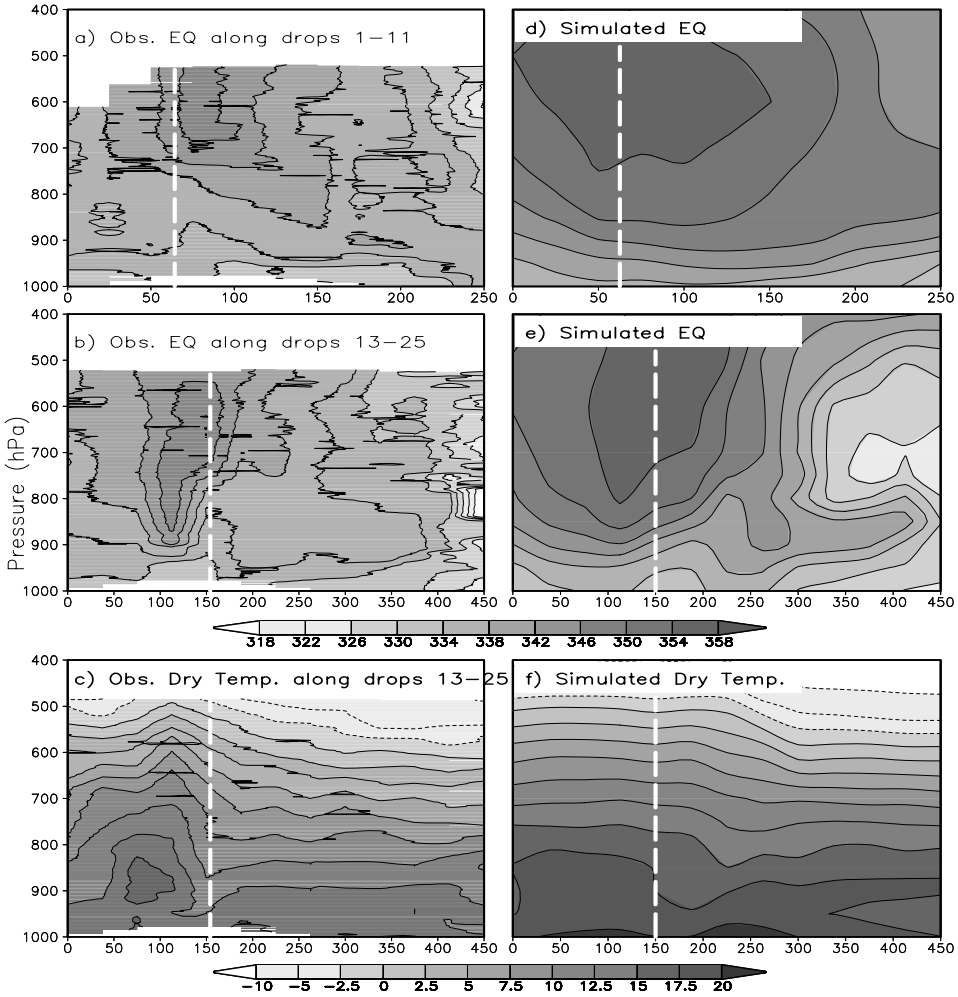

Figure 4. As in Fig. 3, for equivalent potential temperature (denoted as EQ.) in (a) and (b) for observations, (d) and (e) for simulations, (c) and (f) for dry temperature. Dashed line indicates the storm centre.

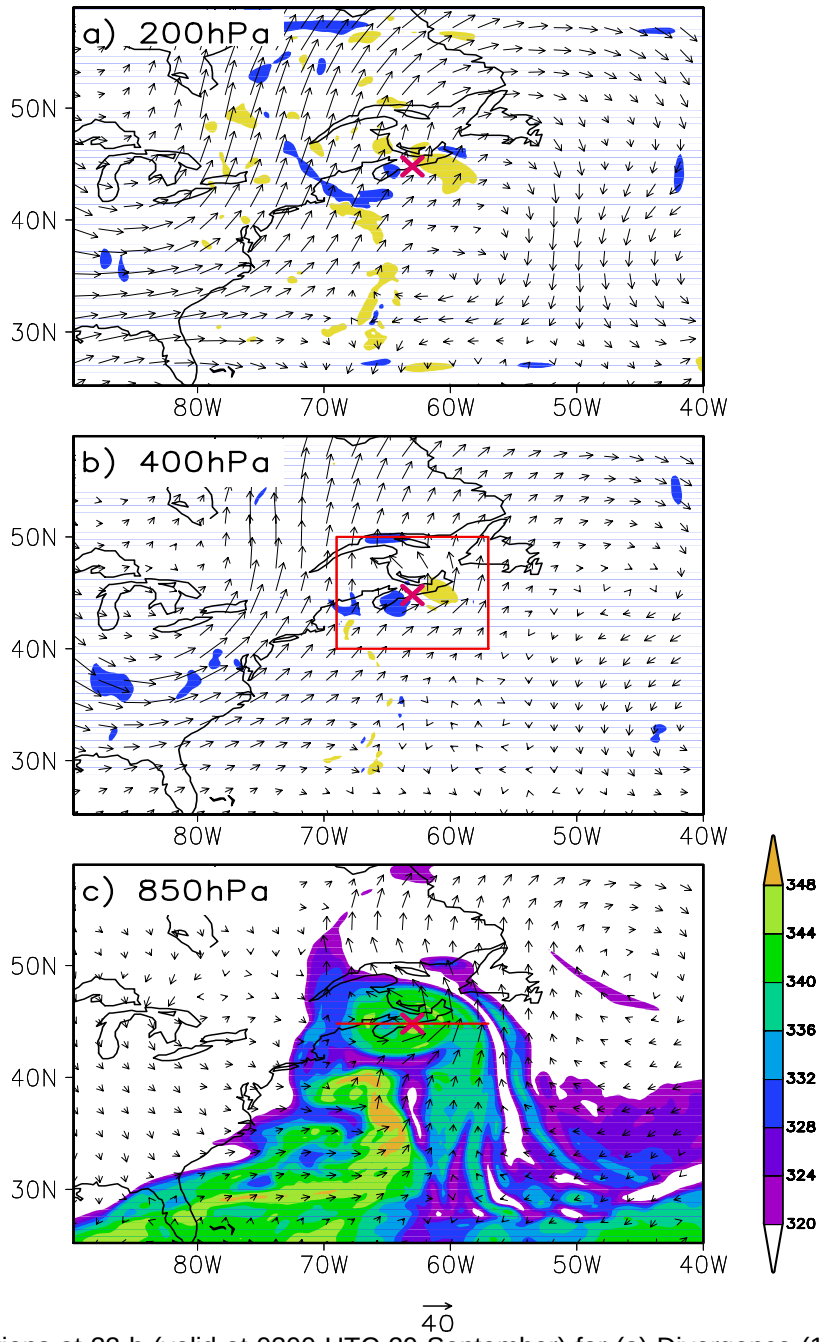

Figure 5. Simulations at 33 h (valid at 0300 UTC 29 September) for (a) Divergence (10^{-5} s^{-1}, above ±5 x 10^{-5} s^{-1} shaded) at 200 hPa, and dark area represents divergence and light area, convergence. (b) Vertical velocity at 400 hPa, and dark area represents ascending motion (more than 0.2 m s^{-1} shaded) and light area, descending motion (less than -0.5 m s^{-1}). (c) θe at 850 hPa. Also superposed is vector wind at each level. The symbol × in each panel marks the location of Juan.

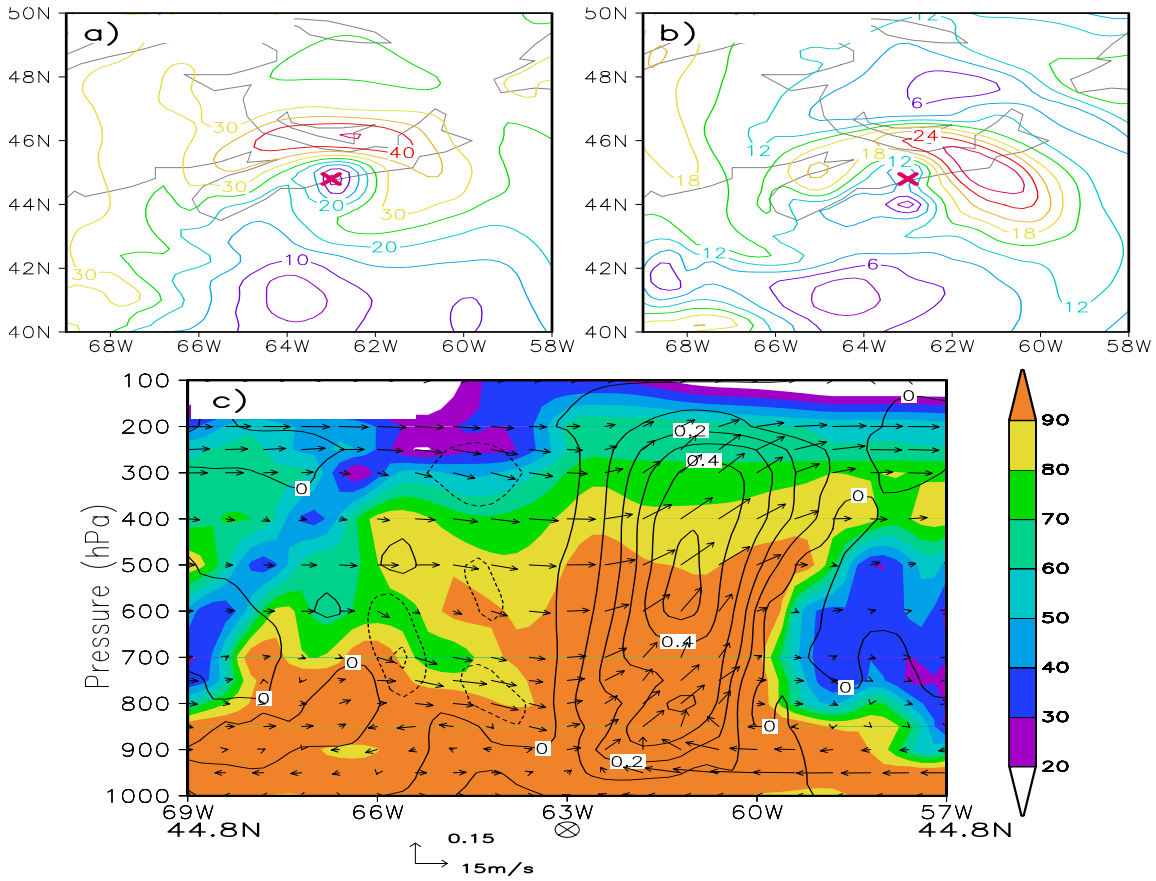

Figure 6. Simulated vertical shear between 850 hPa and 200 hPa for (a), and that between 850 hPa and 400 hPa for (b) at 33 h valid at 0300 UTC 29 September. (c) Vertical cross section of relative humidity (shaded, larger than 80% denotes the cloudiness), vertical velocity (m s^{-1} contour), and along plan flow. Storm center is indicated by symbol X in (a) and (b), ⊗ in (c).